Mineralia Slovaca, Web ISSN 1338-3523, ISSN 0369-2086, https://doi.org/10.56623/ms.2025.57.1.3
57, 1 (2025), 39 – 58, © Authors 2025. CC BY 4.0

3D Long-Term Monitoring of Recent Tectonic Activity in Demänovská Cave of Liberty

MARIÁN STERCZ[1, 2,*], DANIEL GREGA[1, 2], ĽUBOMÍR PETRO[1], PAVEL BELLA[3, 4], JURAJ LITTVA[3], SILVIA JAJČIŠINOVÁ[1] and MARTIN BEDNARIK[2]

[1]State Geological Institute of Dionýz Štúr, Mlynská dolina 1, 817 04 Bratislava 11, Slovak Republic;
[*]marian.stercz@geology.sk, daniel.grega@geology.sk, lubomir.petro@geology.sk, silvia.jajcisinova@geology.sk,
[2]Faculty of Natural Sciences, Comenius University, Ilkovičova 6, 842 15 Bratislava 4, Slovak Republic;
mbednarik@uniba.sk
[3]Faculty of Education, Catholic University in Ružomberok, Hrabkovská cesta 1, 031 04 Ružomberok,
Slovak Republic; pavel.bella@ku.sk
[4]State Nature Conservancy of the Slovak Republic, Slovak Cave Administration, Hodžova 11,
Liptovský Mikuláš, Slovak Republic; pavel.bella@ssj.sk; juraj.littva@ssj.sk

Abstract: The topic of the article is the analysis of recorded data and the presentation of results from almost 24 years of monitoring tectonic movements along a neotectonic fault within the extensive underground space of the Demänovská Cave of Liberty. Displacements and rotations at the fault were measured using a mechanical-optical 3D extensometer TM-71. The measurement results subjected to statistical analysis showed a trend in two components of the spatial motion vector – vertical (Z) and horizontal (Y), which is paralel to the strike of the fault. Recent activity along the fault reflects the action of the contemporary stress field and also seismic activity within the Western Carpathians. The study also examines the relationship between the movements recorded by TM-71 and seismic events in the wider vicinity of the cave. Although long-term measurements show a significant trend of movement along the fault, its magnitude is minimal. From the perspective of cave safety, the detected neotectonic activity does not pose any risk.

Key words: Demänovská Cave of Liberty, Jalovec Fault, recent tectonics, monitoring, 3D extensometer

Graphical abstract

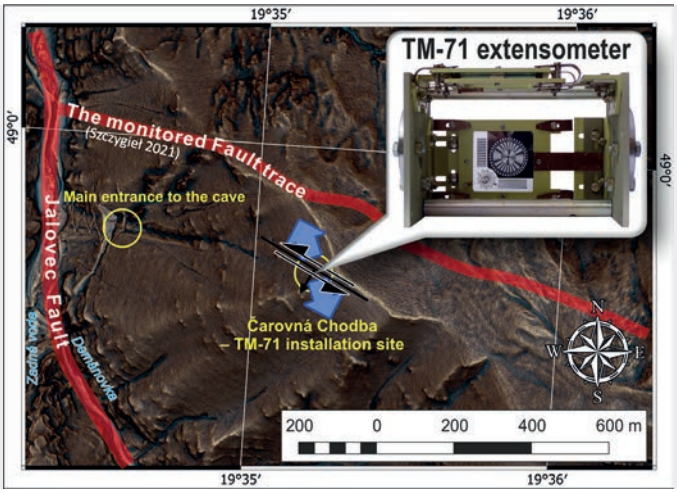

Highlights

- We present results of 3D long-term monitoring of fault activity inside Demänovská Cave of Liberty.
- Trend analyses have been used for data set processing.
- Almost 24 years results have proven permanent but very slow movements along tectonic line.
- Displacements are not continuous but occur in sudden leaps and may be associated with seismic events.

Introduction

Demänovská Cave of Liberty, located in the Demänovská dolina Valley (Nízke Tatry Mts), is a part of the larger Demänová Cave System. It is the longest underground system in Slovakia, and is listed as a National Nature Monument. Its underground spaces are controlled by several tectonic fractures of multiple directions and orientations. The cave was selected in 2001 for 3D monitoring of slow movements along one of the faults due to the occurrence of multiple instances of damage to dripstones (already pointed out by Pokorný, 1952), as well as the neotectonic nature of the faults in the area (Maglay et al., 1999). The start of monitoring is linked to an international project COST-625 *3-D Monitoring of Active Tectonic Structures* solved during the period 2000–2006 (Piccardi, 2006). The site was later included in the national project *Partial Monitoring System – Geological Factors* financed from the budget of the Ministry of the

Environment of the Slovak Republic. Monitoring results are presented in the form of annual reports and are available on the State Geological Institute of Dionýz Štúr (SGIDŠ) website (Ondrus, 2025).

A special 3D extensometer of the TM-71 type with high accuracy (Košťák, 1969, 1991) was chosen to detect displacements on the selected fault. Devices of this type are widely used in Slovakia at a total of 36 locations to monitor not only neotectonic activity on selected faults (e.g. Petro et al., 2004a, b, 2011a; Briestenský et al., 2007, 2011, 2018; Stercz et al., 2025), but also block slope failures (e.g. Petro et al., 1999, 2011b; Wagner et al., 2000; Ondrejka et al., 2014) and historical objects (e.g. Vlčko & Petro, 2002; Petro et al., 2012; Jánová et al., 2021).

The article presents the results of long-term 3D recording of microdisplacements along one of the fault zones in the Demänovská Cave of Liberty, conjugate to the Jalovec Fault, which traverses the axis of the Demänová Valley. The recorded data are subjected to trend analysis, individual phases of neotectonic activity are characterised, and the results are compared with the seismic activity in the broader region.

Location and geology of the study area

The Demänovská Cave of Liberty is situated in the Demänová Valley on the northern slope of the Nízke Tatry Mountains. The valley, approximately 10 km in length

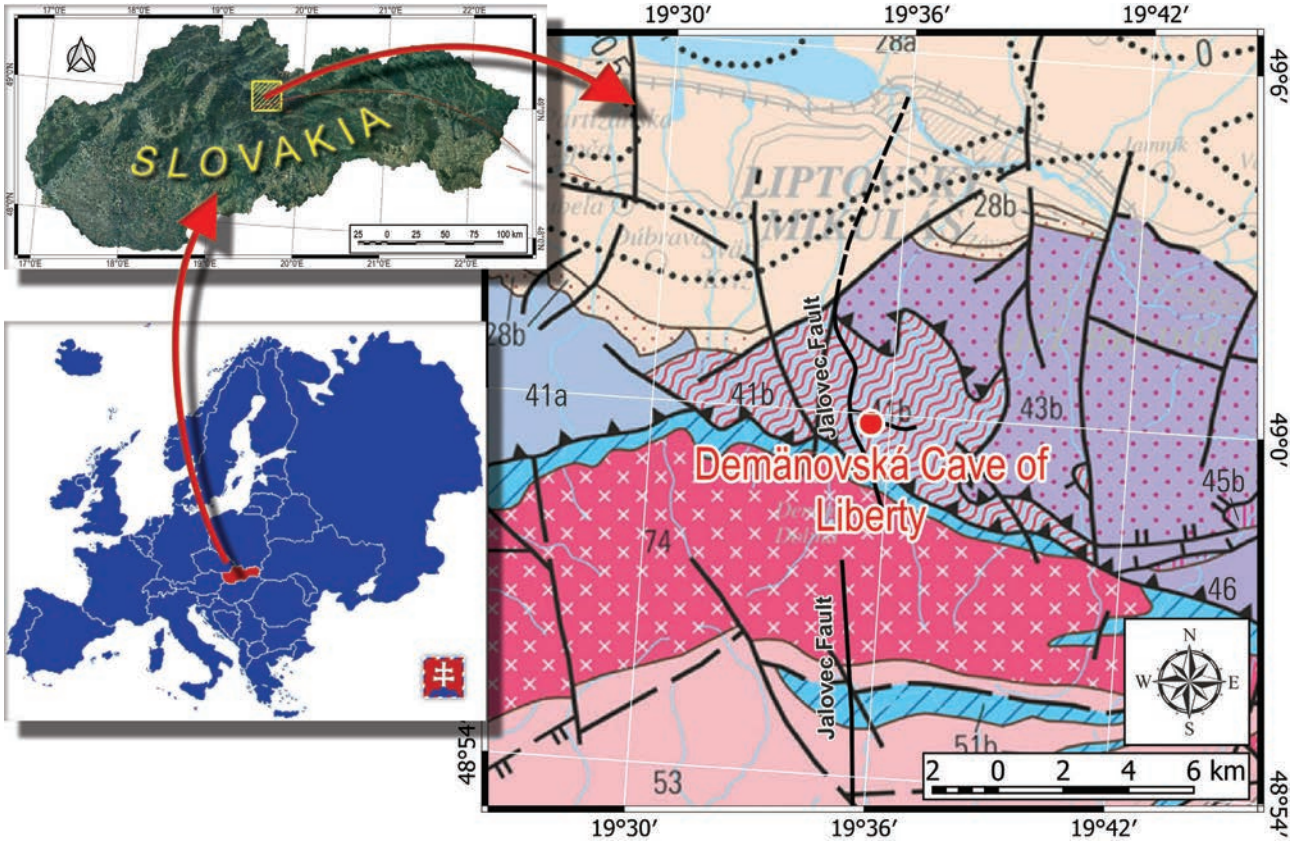

Fig. 1. Excerpt from the Tectonic Map of Slovakia showing the area around the Demänovská Cave of Liberty (Bezák et al., 2004). Neo-Alpine tectonic structures of the Inner and Outer Western Carpathians include sedimentary basins filled with Paleogene and Upper Cretaceous sediments: 28 – Intra-Carpathian extensional basins in the back-arc setting (Middle Eocene–Lower Miocene): a) deep-water sediments of the outer shelf, slope, and oceanic plateaus; b) shallow-marine shelf sediments. Paleo-Alpine tectonic units of the Inner Western Carpathians comprise the following: Fatricum – 41: a) Mesozoic formations with deep-water sediments (Jurassic–Lower Cretaceous); b) Mesozoic formations with shallow-marine sediments (Jurassic–Lower Cretaceous); c) clastic Permian sediments. Hronicum – 43: nappes formed from Triassic intraplatform basins (Biely Váh-type development): b) from the Biely Váh-type basin; 45: nappes formed from Triassic carbonate platform (Čierny Váh-type development): b) from the Čierny Váh-type carbonate platform; 46: clastic and volcanic sequences of the Carboniferous–Lower Triassic. Tatricum – 51: cover formations (Upper Paleozoic–Middle Cretaceous): a) Mesozoic formations with deep-water sediments (Jurassic–Lower Cretaceous); b) Mesozoic formations with shallow-marine sediments (Jurassic–Lower Cretaceous); c) Upper Paleozoic clastic sediments. Hercynian tectonic units in the crystalline basement (Proterozoic?–Paleozoic) – 53: upper lithotectonic unit (originally high-grade metamorphic paragneisses, amphibolites, migmatites, and orthogneisses – mainly Paleo-Hercynian granitoids). Meso-Hercynian collisional granitoids – 74: suite of I-type granitoids (crust-mantle granitoids dominated by granodiorites and tonalites, Devonian–Lower Carboniferous).

and pear-shaped in outline, is bordered by the following elevations: Demänovská Poludnica (1 304.3 m), Magura (1 376.4 m), Krakova hoľa (1 750.6 m), Krúpova hoľa (1 927.2 m), Chopok (2 023.3 m), Poľana (1 873.0 m), Siná (1 559.6 m) and Opálenisko (1 143.3 m). Its morphological character is primarily conditioned by the geological structure and tectonic framework of the area.

The Nízke Tatry Mountains are composed of three tectonic units – Tatricum, Fatricum, and Hronicum (Biely et al., 1997). The Ďumbier segment of this range, where the Demänová Valley belongs, is situated within the Tatra–Fatra zone of the Inner Western Carpathians' core mountains.

The valley was formed by the Demänovka Stream and its tributaries. Its upper (southern) parts on the Tatricum crystalline basement display fluvial and glacial landforms, while the lower (northern) section is featured by fluviokarst landforms, monoclinal morphostructures and sharply arched carbonate ridges and cliffs (Droppa, 1972). The Demänovská Cave of Liberty is the most significant section of the multi-level Demänová Cave system, with a currently known total length exceeding 51 km (Slovak Speleological Society, 2025). It was formed by sinking allochthonous waters of the Demänovka and Zadná voda streams in the Triassic limestones of the Fatricum (Krížna Nappe), which overlies the Tatricum crystalline basement and its sedimentary cover from the north (Fig. 1).

The faults and joints controlled the valley's position and directed watercourses, significantly influencing the shaping of the surface relief of the Demänová Valley. These faults thus guided the origin and development of the Demänovská Cave System and other karst features (Droppa, 1972).

The cave passages and chambers, formed mostly in the Middle Triassic Gutenstein Formation of the Fatricum, are aligned along two fracture systems oriented NW–SE and NE–SW (Droppa, 1957, 1972). The principal fault system traversing the axis of the Demänová Valley is the Jalovec Fault (Hók et al., 2000), which trends N–S (to the north) and NNW–SSE (to the south of the site) in the vicinity

Fig. 2. Damaged speleothem decorations in the underground passages of the Demänovská Cave of Liberty. The TM-71 extensometer is visible in the bottom right photograph (Čarovná chodba Passage – photo by M. Stercz).

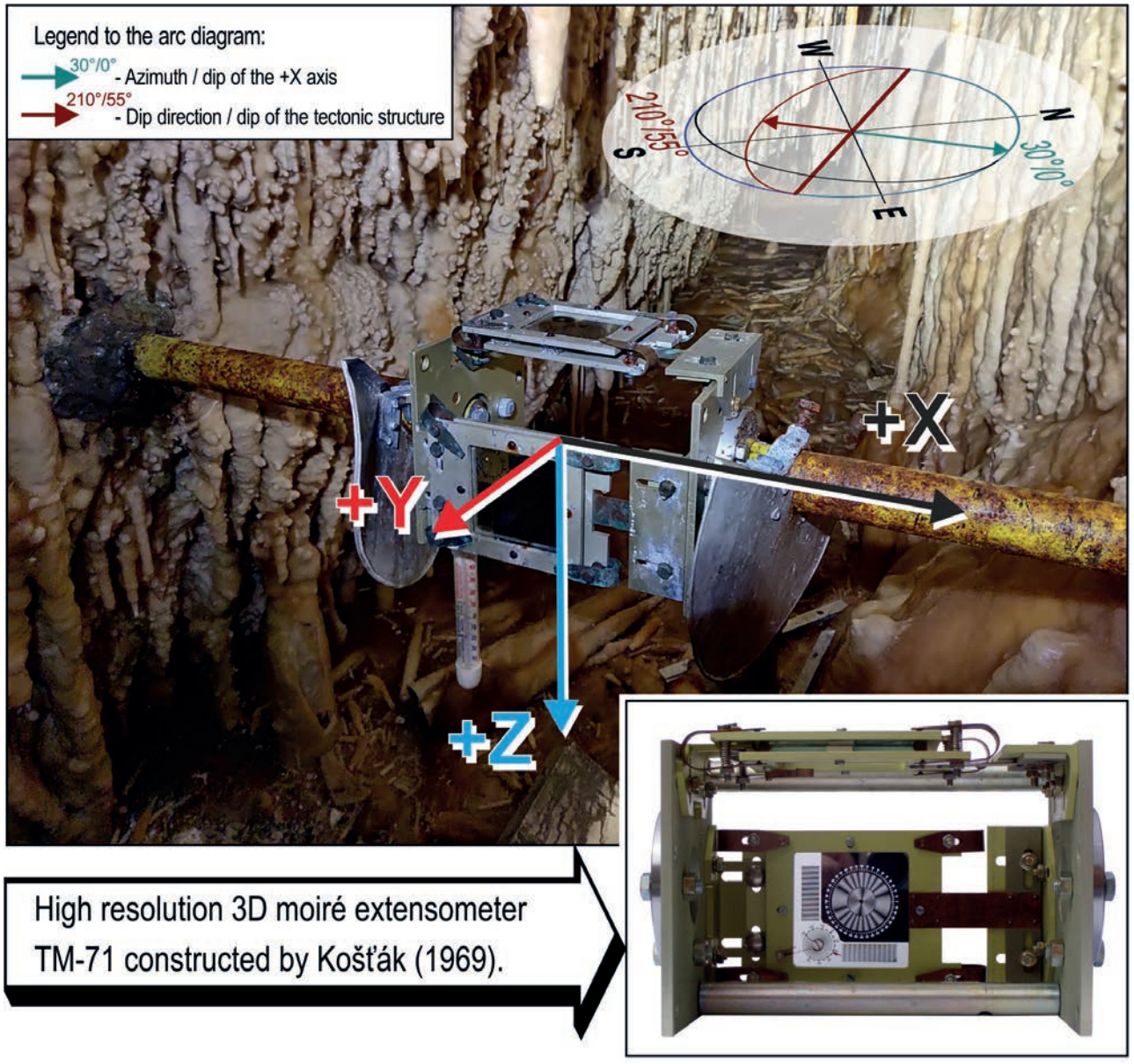

Fig. 3. Installation of the TM-71 mechanical-optical extensometer in the Čarovná chodba Passage of the Demänovská Cave of Liberty (photo by Ľ. Petro).

of the monitored site. The monitored fault direction is WNW–ESE and is conjugate to the aforementioned fault system.

The TM-71 extensometer was installed in the so-called Čarovná chodba Passage, which developed through corrosive widening of this fault under phreatic conditions, with minimal evidence of fluvial modification (Bella et al., 2014; Bella, 2016).

The aim of installing the TM-71 device in the Demänovská Cave of Liberty was to determine whether the tectonic processes that contributed to the cave's formation are still active today. In the Čarovná chodba Passage – the site of the instrument's installation – macroscopic evidences of neotectonic movements were observed, including fractures and cracks in speleothems (Petro et al., 2004b; Briestenský et al., 2010), as well as numerous broken stalactites and stalagmites of varying size and age (Fig. 2). The TM-71 extensometer was intended to confirm and quantify the magnitude of these movements, and to define their attributes – direction, rate, and character.

The Čarovná chodba Passage, where the instrument was installed at the end of August 2001 (Fig. 3), was formed, as previously mentioned, by the activity of groundwater in a structurally weakened zone aligned in a WNW–ESE direction (with a general fault dip orientation of 210°/55°). The X-axis of the device points NE and represents the

installation orientation. The monitored fault dips towards the SW at an angle of 55°, and to some extent reflects the inclination of the terrain surface.

Data readings at this site are not recorded automatically but are instead taken manually, with the assistance of staff from the Slovak Caves Administration (SCA). Since the installation of the device, a total of 81 measurements have been taken to date, at intervals of approximately three to four months (3–4 readings per year).

Methodology of Data Acquisition and Processing

Based on the data measured so far, the movement along the monitored fault is not particularly significant. Over a period of 24 years, its magnitude has ranged from hundredths to tenths of a millimetre. If the instrument had been installed on the surface rather than underground – where it would be exposed to more pronounced climatic factors – it probably would not have been possible to evaluate the data reliably, as the distortion caused by external factors would greatly exceed the measured manifestations of neotectonic movements. In this case, however, the climatic conditions within the cave are highly stable, and therefore the measured data – regardless of their small magnitude – can be considered valid.

At small magnitudes of recorded microdisplacements, the sensitivity of the instrument is critical to the usability of the data. The minimum detectable displacement – i.e. the lower detection threshold – is determined by the physical principle of measurement and the characteristics of the applied moiré grating (Rowberry et al., 2016). For the instrument currently in use, the standard uncertainty of Type B associated with its construction can be estimated in accordance with the principles outlined in the Guide to the Expression of Uncertainty in Measurement (GUM) (BIPM et al., 2008), using the following general expression:

$$u_B = \frac{Z_{max}}{\sqrt{3}}$$

where Z_{max} denotes the maximum possible deviation due to the instrument's resolution or design limitations – in this case, equal to the smallest division of the instrument's scale, i.e. its resolution (1 moiré fringe = 0.05 mm).

$$u_B = 0.029\ mm$$

This value refers to the length of the displacement vector in the measured plane, expressed in polar coordinates. When converted to Cartesian coordinates, the instrument's minimum resolution becomes a function of the angle (sine or cosine) between the projection of the spatial displacement vector in the analysed plane and the respective axis of the coordinate system. As a result, the minimum resolution when using the manual fringe-counting method may vary within the interval $< 0; 0.029 >$ mm.

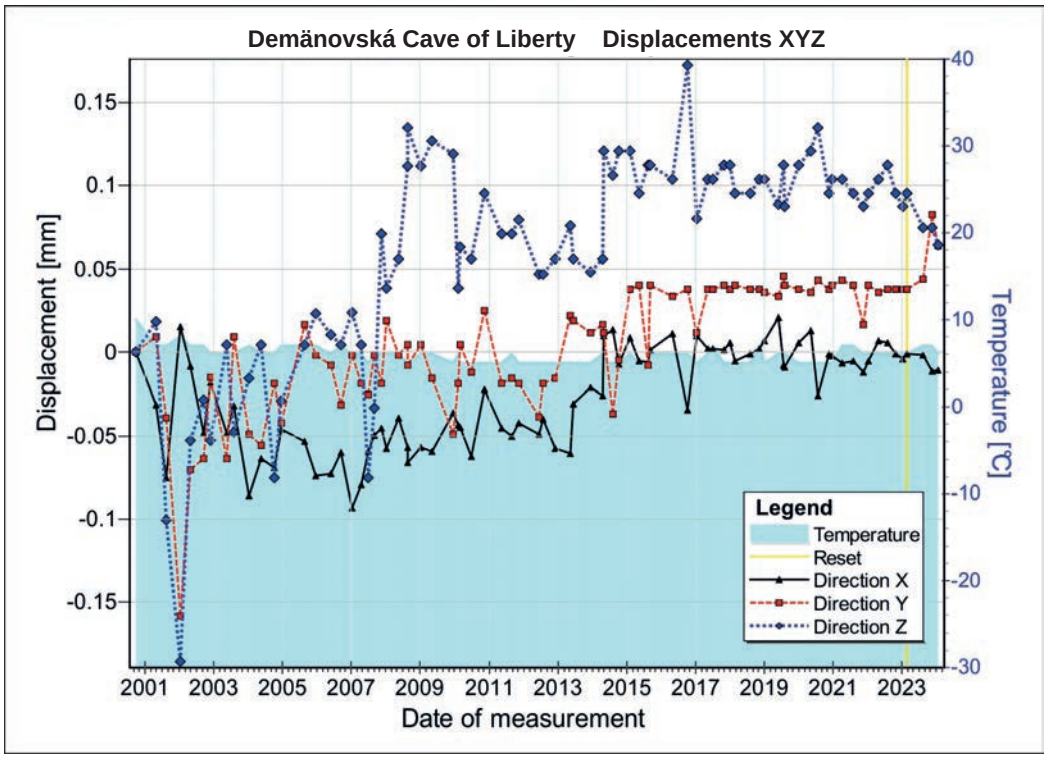

Fig. 4. Representation of measured displacement data in a 2D graph – graphical output from the MSDilat software.

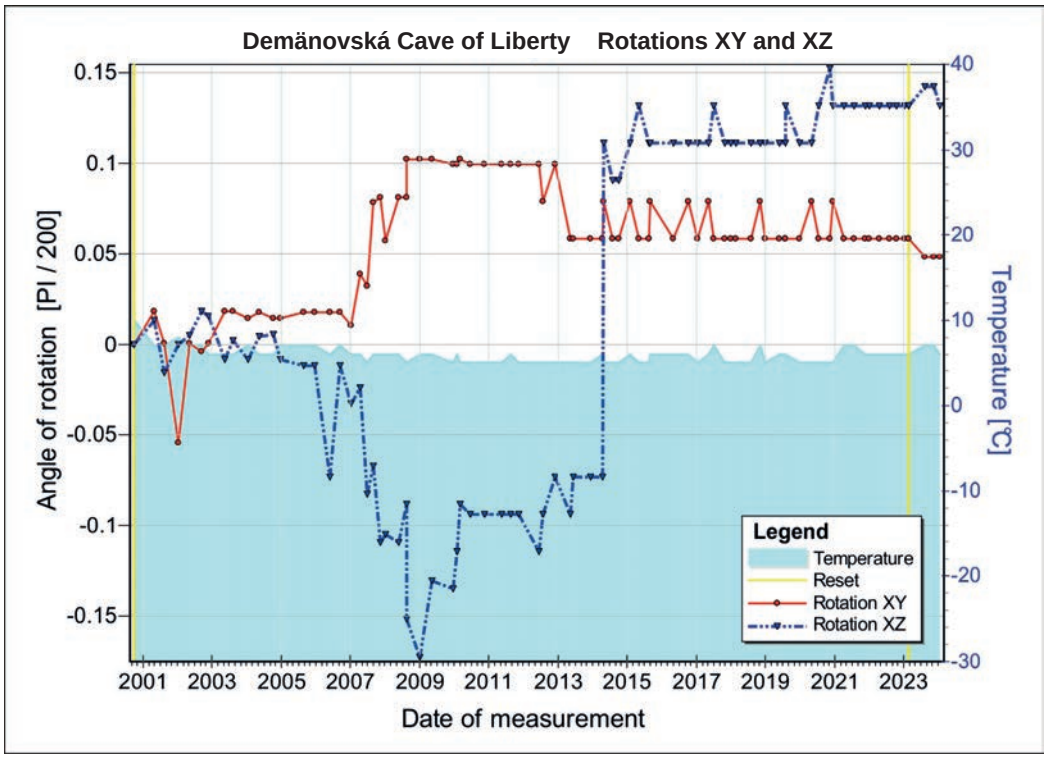

Fig. 5. Representation of measured rotation data in a 2D graph – graphical output from the MSDilat software.

In Table 1, the values marked with an asterisk (*) represent data points that are either at the threshold of the instrument's detection capability or fall below the detection limit, indicating minimal or undetectable movement.

The measured data were converted into units of length (for microdisplacements) and angular degrees (for rotations) using the MSDilat software (Stercz, 2021). Figs. 4 and 5 show 2D graphs of displacement and rotation. The displacement graph displays the decomposed spatial vector of movement into X, Y, and Z directional components over time. Rotations represent the tilting of monitored rock blocks relative to each other within the XY plane (horizontal) and the XZ plane (vertical, perpendicular to axis Y).

Table 1 presents the data recorded during the entire monitoring period. For simplicity and clarity, values in each direction were aggregated by calendar year – producing so-called interval time series, thereby partially removing seasonal variations. The index indicates the identified yearly measurements used in graphical representations in the three fundamental orthogonal planes.

The process of calculating the geographic parameters of motion and interpreting the data in the horizontal plane is illustrated in Fig. 6. The angle α for each partial motion vector represents the angle between the horizontal projection of the vector and the X-axis direction in the TM-71 coordinate system (the formula is shown in the figure). The resulting azimuth δ is calculated as the sum of α and β, where β is the horizontal deviation of the instrument's axis from geographic north. At the Demänovská Cave of Liberty site, the resulting direction of horizontal movement in the instrument coordinate system over the entire monitoring period is α = 99.5°. Since the +X axis is offset by β = 30° from geographic north, **the calculated geographic azimuth of horizontal movement is δ = 129.5°.** This indicates that in the horizontal plane, the mobile block shifts in the NW–SE direction, with the total movement over the entire monitoring period amounting to only about 0.065 mm (rounded to three decimal places).

In the following two figures (Figs. 7 and 8), the procedure for calculating the movement direction in the vertical plane – i.e. the values of angles λX and λY for the vertical, mutually perpendicular planes XZ and YZ – is illustrated schematically (Fig. 7 – XZ plane; Fig. 8 – YZ plane). These values represent the dip magnitude (i.e. the deviation of the resultant movement vector from the horizontal plane) as viewed from the XZ or YZ plane, respectively. The calculation principle, along with the mathematical formulae, is shown in the figures. The actual resultant dip is a combination of dips in both vertical planes and can be calculated using the following formula:

$$\lambda = arctan \frac{\Delta Z}{\sqrt{\Delta X + \Delta Y}} * 180/\pi$$

The resultant dip of the motion vector at the Demänovská Cave of Liberty over the entire monitoring period is, after rounding, λ = 45°.

Tab. 1

Measured and calculated data for individual years of monitoring

Measurements			Displacements			Rotations	
INDEX	Year of	Number of	X	Y	Z	XY	XZ
1	2001	1	0.000	0.000	0.000	0.000	0.000
2	2002	3	0.015	–0.158	–0.186	–0.051	0.011
3	2003	3	–0.018	–0.015	–0.053	0.003	0.027
4	2004	3	–0.086	–0.049	–0.016	0.017	0.003
5	2005	3	–0.046	–0.042	–0.029	0.017	0.003
6	2006	2	–0.074	–0.002	0.023	0.021	0.000
7	2007	3	–0.094*	–0.002	0.024	0.013	–0.021
8	2008	5	–0.058	0.019	0.039	0.060	–0.093
9	2009	4	–0.057*	0.005*	0.112	0.106	–0.161
10	2010	2	–0.036	–0.049	0.119*	0.103	–0.123
11	2011	4	–0.022	0.025	0.096*	0.103	–0.082
12	2012	3	–0.042	–0.019	0.079*	0.103	–0.082
13	2013	3	–0.057*	–0.015*	0.056*	0.103	–0.062
14	2014	3	–0.021	0.011	0.048	0.062	–0.062
15	2015	5	0.009	0.038	0.121	0.082	0.123
16	2016	3	0.001*	0.040*	0.112*	0.082	0.123
17	2017	3	0.010*	0.011*	0.080*	0.062	0.123
18	2018	4	0.005*	0.038*	0.112*	0.062	0.123
19	2019	4	0.007*	0.036*	0.104*	0.062	0.123
20	2020	4	0.005*	0.038*	0.112*	0.062	0.123
21	2021	4	–0.002*	0.040*	0.104*	0.082	0.144
22	2022	4	–0.005*	0.040*	0.096*	0.062	0.144
23	2023	4	–0.004*	0.038*	0.087*	0.062	0.144
24	2024	4	–0.011*	0.064*	0.065*	0.051	0.144

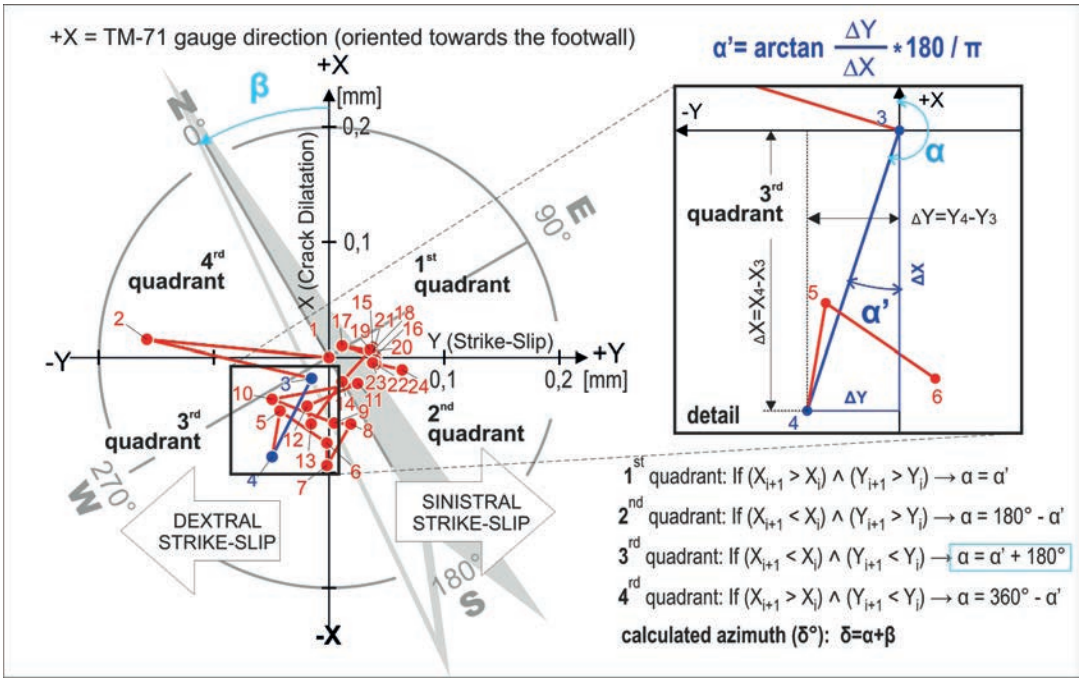

Fig. 6. Schematic representation of movement direction calculation in the horizontal XY plane (adapted from Briestenský et al., 2018).

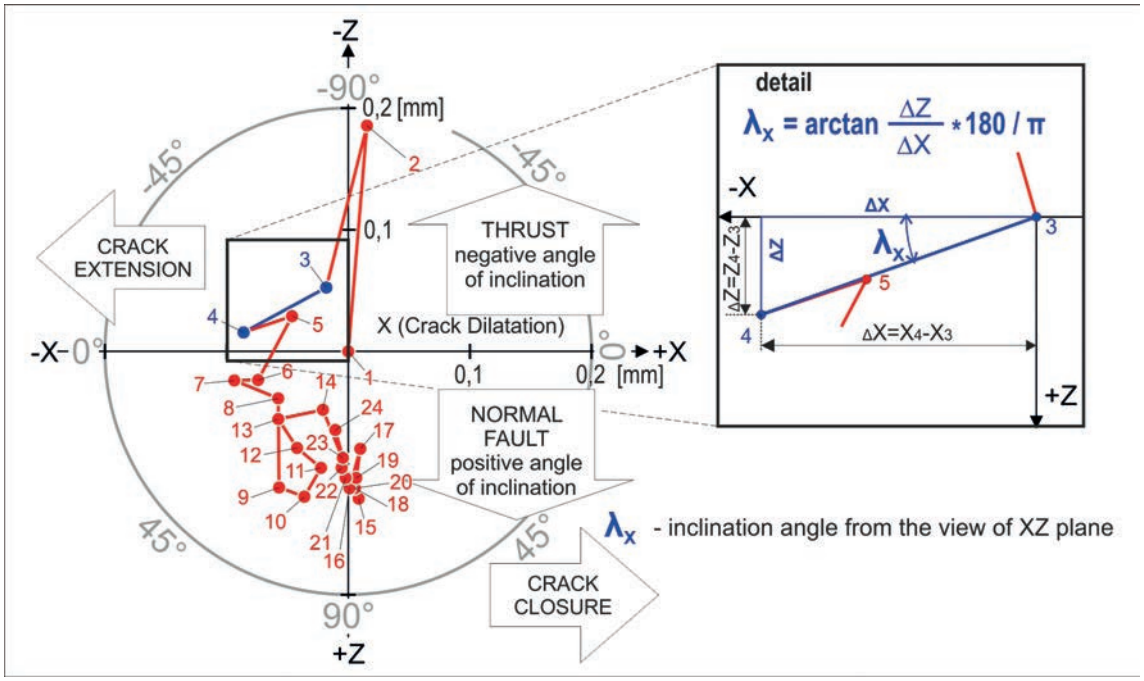

Fig. 7. Schematic representation of dip λX calculation (movement direction in the vertical XZ plane; adapted from Briestenský et al., 2018).

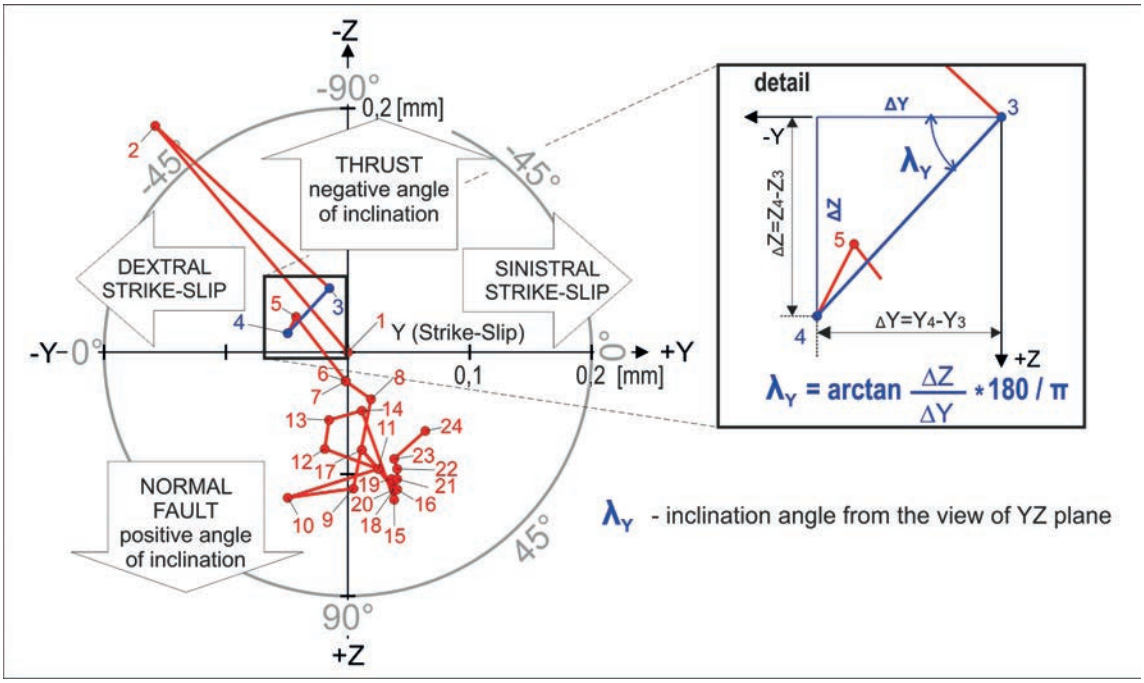

Fig. 8. Diagram of the calculation of dip angle λY (direction of movement in the vertical YZ plane; adapted from Briestenský et al., 2018).

The magnitude of the motion vector is representing the total displacement over the monitored period (from August 2001 to December 2024).

It represents the vector sum of the measured movements in the horizontal and vertical planes. It can be calculated according to the formula:

$$|XYZ| = \sqrt{|XY|^2 + |Z|^2}$$

where |XY| is the magnitude of the movement in the horizontal plane, calculated using the formula:

$$|XY| = \sqrt{|X|^2 + |Y|^2}$$

The magnitude of the total motion vector is 0.092 mm. When decomposed into individual components |X|, |Y|, and |Z|, it can be stated that the Y and Z components contribute almost equally to the total magnitude of the movement vector – each accounting for more than 45 % – while the X component contributes only marginally, less than 8 %. In summary, the detected movement along the tectonic structure may be described as a minor sinistral (left-lateral) displacement with a slight subsidence of the SW block, accompanied by a tendency for the fault to open. Calculated values of all the components are given in Table 2.

Tab. 2

Calculated values of the components of the total motion vector

Component of motion vector	|X|	|Y|	|Z|	|XY|	|XYZ|
Magnitude of movement [mm]	0.011	0.064	0.065	0.065	0.092

The representation of the individual measured motion vectors on a spherical surface in the form of a tectonogram is shown in Fig. 9. The diagram also includes the installation parameters of the instrument (in turquoise color) – azimuth of the X-axis: 30°, and its dip: 0°. Similarly, structural data of the monitored fault are displayed – dip direction and dip (210° / 55°), along with the resultant direction of movement derived from the data – the horizontal projection of the spatial vector and its inclination from the horizontal plane (129° / 45°).

Unlike a standard tectonogram, where data are plotted using stereographic projection only on the lower hemisphere (as dip angle ranges from 0° to 90°), data in this diagram may be plotted on both hemispheres since the dip of the movement vector can be positive (downward) or negative (upward), ranging from –90° to +90°. Measurements plotted on the lower hemisphere are shown in red, those on the upper hemisphere in green.

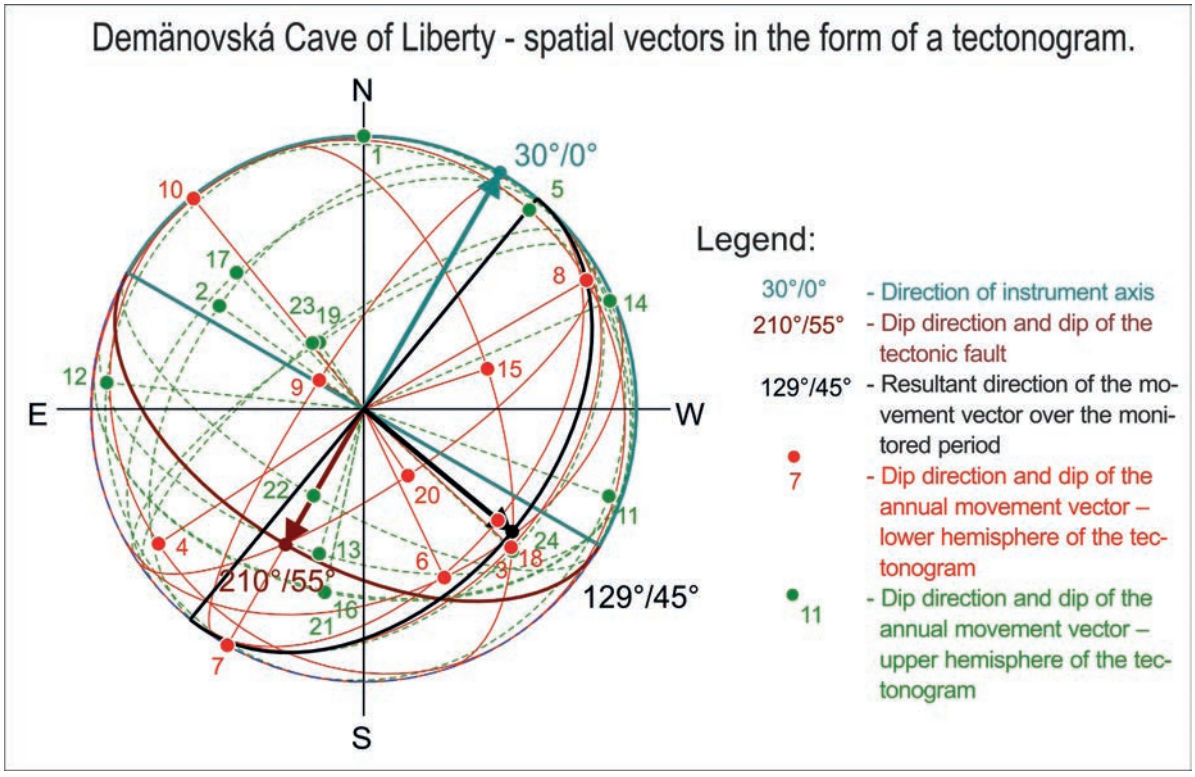

Fig. 9. Display of spatial vectors of aggregated annual measurements in the form of a tectonogram.

Aggregated values for each calendar year are plotted, with the adjacent number corresponding to the index used to identify the measurement in Table 1. An examination of the diagram shows that the measured data exhibit a slight predominance of movements with steep inclinations (points located closer to the centre of the diagram) and a prevailing NW–SE orientation. The number of upward-directed measurements is comparable to those directed downward, indicating that no significantly dominant movement occurs in either direction within the vertical plane.

In order to evaluate microdisplacements relative to the fault being monitored, the instrument installation parameters and the structural attributes of the fault must be carefully recorded. Although the TM-71 can measure movements in any general direction, it is recommended to install it following standard principles to simplify calculations. Typically, the device is mounted so that the X-axis, if possible, is horizontal and aligned with the direction of opening or closing of the fault (i.e. along the dip azimuth), and the Y-axis is perpendicular to the dip direction and always horizontal. Installation data are recorded and considered during evaluation in the processing software. In the case of the Demänovská Cave of Liberty site, the instrument was installed in accordance with standard practice, with the X-axis aligned with the

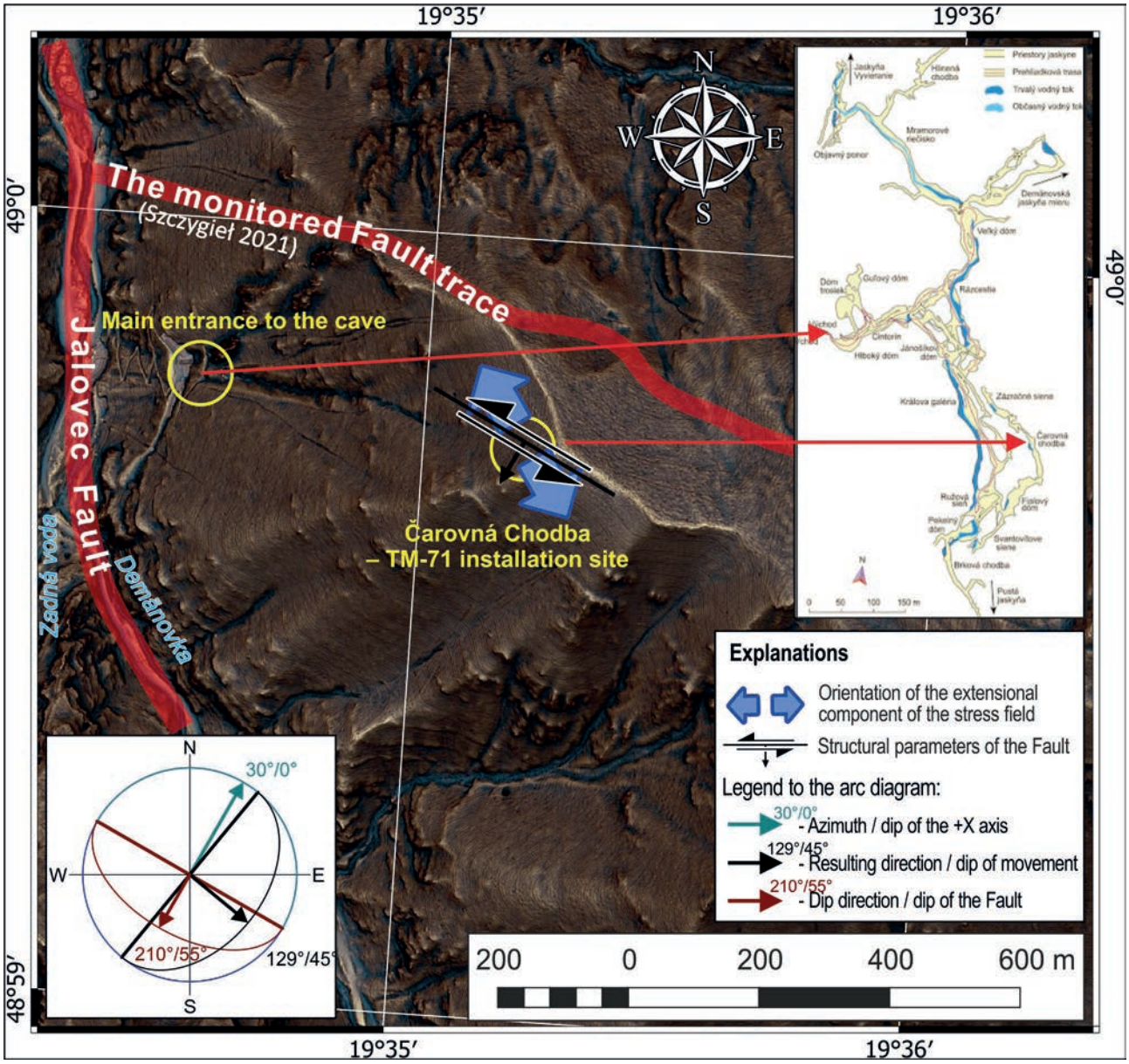

Fig. 10. Surface projection of the TM-71 instrument installation site, showing its orientation.

dip direction of the monitored fracture. Both X and Y axes lie in the horizontal plane, +Z points downward, and the +X direction points toward the assumed stable block of the monitored fault line. The surface projection of the TM-71 instrument installation site is shown in Fig. 10, illustrating its orientation, the orientation of the fault, and the resulting direction of the movement vector. By entering the measured data into the structural geological software GS2PS (Sasvári & Baharev, 2014), the orientation of the extensional component of the stress field was calculated and is illustrated in the figure.

Assuming that the source of the monitored activity in the rock mass is a regionally persistent (monotonic) recent neotectonic process (RNP) over the duration of the monitoring, this should manifest as a continuous and long-term consistent movement along the fault, characterised by a distinct trend component in the time series. To verify this assumption, trend analysis is appropriate.

Trend Analysis of the Measured Data

When the measured data from the TM-71 are arranged chronologically, they form a time series for each component of the motion vector. The aim of analysing these datasets is not only to determine whether any movements are occurring along the tectonic line, but also to identify whether such movements exhibit a definable long-term trend potentially associated with neotectonic processes. In this case, the statistical analysis of microdisplacement trend curves was employed to confirm or refute the hypothesis of a long-term trend in the measured movements, which could indicate the nature of the stress regime within the rock mass over an extended time frame.

For the trend analysis, the non-parametric Mann-Kendall (MK) trend test (Mann, 1945) was applied in combination with Sen's method for calculating the slope of the regression line (Sen, 1968). The trend analysis was applied to the primary data, aggregated into time series

Tab. 3

Results of trend analysis of the measured values at the Demänová site

Demänová – statistical trend analysis of TM-71 microdisplacement and rotation curves					
Tested time series	**Microdisplacement**			**Rotation curves in XY a XZ planes [π/200]**	
	X	**Y**	**Z**	**XY**	**XZ**
MK-test statistics	**Mann-Kendall test (MK-test)**				
n	24	24	24	24	24
α	0.05	0.05	0.05	0.05	0.05
S	78	177	124	69	121
Var(S)	1	1	1	1	1
σ	40.291	40.112	40.183	39.594	39.804
Zs	1.960	1.960	1.960	1.960	1.960
p	0.05599	0.00001	0.00221	0.08590	0.00257
Trend	**NO**	**YES**	**YES**	**NO**	**YES**
SM statistics	**Sen's method**				
α	–	0.05	0.05	–	0.05
N	–	276	276	–	276
k	–	78.619	78.757	–	78.014
β	–	0.0035	0.0058	–	0.007
β-lower	–	0.002	0.003	–	0.003
β-upper	–	0.006	0.009	–	0.011
Δd[mm] | Δφ[π/200]	–	0.084	0.140	–	0.169
Δd | Δφ – lower	–	0.056	0.067	–	0.072
Δd | Δφ – upper	–	0.132	0.209	–	0.252

n – number of observations; α – significance level; S – Mann-Kendall test statistic; Var(S) – variance of the S statistic; σ_s – standard deviation of S; Z_s – standardised test statistic (positive values indicate an increasing trend, negative values a decreasing trend); p – p-value (statistical significance of the trend); k – rank index used for calculating the confidence interval of the slope; β – Sen's slope (estimated median slope of all pairwise data combinations); Δd [mm] / Δφ [π/200] – estimated displacement per unit time in the horizontal (Δd) and angular (Δφ) component

with an interval length of one year (Tab. 1). The results for the individual time series are summarised in Table 3. The following findings emerged from this statistical analysis:

- A statistically significant trend at the 95 % confidence interval was demonstrated in the examined primary datasets of displacements in the Y and Z directions.
- For the data representing movement along the X axis, no statistically significant trend was confirmed.
- In the datasets of measured movements in Y and Z directions, the trend is positive (the statistical value of the MK test $S > 0$); the implications of the direction of the curves in relation to their geographic orientation are described further in the subchapter *Characteristics of the Curves*.
- Based on the p-value, which expresses the probability of rejecting the null hypothesis (the null hypothesis H_0 assumes no trend exists in the tested dataset), the reliability of trend detection is highest in the Y direction – that is, for horizontal displacement perpendicular to the direction of the instrument's installation (p-value << significance level $\alpha = 5$ %).

In the datasets of measured rotations, the presence of a trend is less reliable. The curve representing rotation in the XY plane does not show a trend, and the measured data appear random and independent. For the XZ curve, the presence of a trend is demonstrated based on the p-value, although the level of reliability is somewhat lower than that of the Y curve. As with the other curves, the trend in this case is also positive.

If a statistically significant trend is confirmed, its magnitude can be determined using the Sen coefficient – the slope of the trend line β (Tab. 3). Sen's method (Sen, 1968) assumes a linear trend within time series data, which is generally expected in long-term observations of fault movements. In reality, however, the release of stress in rock masses rarely occurs smoothly in the short term. It typically manifests as short episodes of temporary changes in measured parameters, which may be associated with other indicators of tectonic activity, such as seismic events.

Although tectonic activity in the Demänovská Cave of Liberty can be considered relatively stable over the monitored period, certain time intervals can still be identified that display a similar character in monitored indicators (see interpretation below). This reflects how accumulated stress in the rock environment is released over time. For example the data clearly show that activity of displacements along the monitored fault was most pronounced up to the end of 2015. From the beginning of 2016, however, this activity significantly decreased and remained subdued until the end of 2024. It should be noted, that the same period of tectonic inactivity was observed also at other monitored sites (Hochmuth et al., 2020).

Characteristics of Measured Components

The data outputs from the TM-71 instrument installed in the Demänovská Cave of Liberty are in the form of time series. The X, Y, and Z components represent the spatial characteristics of the 3D vector of relative movement between blocks along the fault, while XY and XZ denote their mutual rotation in two orthogonal planes.

X-Component of the Movement Vector

The X-component corresponds to horizontal movement in the dip direction of the tectonic fault. Based on the geometry of the instrument's installation, this component indicates the opening or closing of the gap between the measured blocks. According to the trend analysis, the X-component data did not exhibit a statistically significant trend. The curve initially shows a downward trend (fault opening) until the end of 2007, followed by an upward trend until mid-2015 (fault closing). In the years following, the curve stagnates or shows a slight decrease.

The curve is relatively irregular – though this term is used cautiously due to the very low magnitude of changes between readings. The measured values fluctuate around the mean with an average amplitude of 0.02 mm, which is near the detection limit of the instrument. The highest annual displacement in the X direction was recorded in 2004, at only 0.068 mm. The net change over the entire monitoring period is 0.01 mm, with a total range of 0.115 mm.

In such cases, the statistically adjusted average value is more meaningful than individual measurements. Nonetheless, individual readings may be relevant in connection with seismic events, where sudden displacements on the fault may be indicative of specific earthquakes (see: Measurement Interpretation).

Y-Component of the Movement Vector

This component reflects horizontal movement along the fault, where positive values (+Y) indicate sinistral (left-lateral) displacement, and negative values indicate dextral. Based on the MK test, the Y curve demonstrates a statistically significant positive (increasing) trend, with an average annual increment slope $\beta = 0.0035$ mm. However, immediately after installation in August 2001, the trend was negative ($\beta = -0.18$ mm), and it shifted sharply to an increasing trend only at the end of 2002, which persisted until the end of the monitored period. As with the X-component, this curve is characterised by sudden shifts alternating with longer stable periods. The data fluctuate around the mean with a slightly higher amplitude of up to 0.04 mm. The overall range over the full

period is slightly greater (0.24 mm), with the maximum annual displacement reaching 0.158 mm. The net change over the entire period is 0.064 mm.

Z-Component of the Movement Vector

Movement along the Z-axis reflects the vertical component of displacement. If the X-axis points toward the stable block (i.e. the presumed immobile side of the fault) and the +Z axis points downward (as is the case here), positive Z values indicate subsidence of the moving block, while negative values represent uplift or reverse faulting. Like the Y-component, the MK test confirms a statistically significant increasing trend. The full range of measured values spans from –0.186 mm to +0.173 mm.

During the first year of measurement, the Z-component had a similar pattern to the Y-component. An initial downward trend transitioned sharply to an upward trend, which persisted in subsequent years. From April 2015, a gradual stagnation or slight decline was observed. The final value of the Z-component over the full monitoring period is positive at 0.065 mm.

Measurements of rotations

As previously mentioned, the TM-71 instrument can detect rotations – mutual angular displacements between measured blocks in the horizontal (XY) and vertical (XZ) planes. These values are sensitive to stress changes in the rock mass along the fault and may also reflect short-term geodynamic pulses or seismic events.

Although trend analysis confirmed a statistically significant trend in XZ-plane rotations over the entire monitoring period, this indicator has limited spatial relevance since rotational displacement between blocks is not expected to increase indefinitely in one direction. More crucial are short-term changes in trends, which indicate shifts in the mechanics of force and stress distribution within the rock mass. At the Demänovská Cave of Liberty site, several such moments can be identified in the rotation curves. At the end of 2007, a change in trend occurred in both rotation curves, lasting for approximately two years. Afterwards, XY-plane rotations stagnated for four to five years, while XZ-plane rotations showed an increasing trend. In spring 2015, a sudden change in the XZ rotation by 0.2° was recorded, representing a significant shift. No further major changes were observed in the rotation data: the XY rotation curve remained stable, and the XZ curve showed only a slight increase. Total rotation in the horizontal plane did not exceed 0.1°, while in the vertical plane (dip direction of the fault), the range was approximately 0.3° (from –0.15° to +0.15°).

Seismic Events

Despite the lack of historical records of major seismic events in the area, it is assumed that extensive damage to

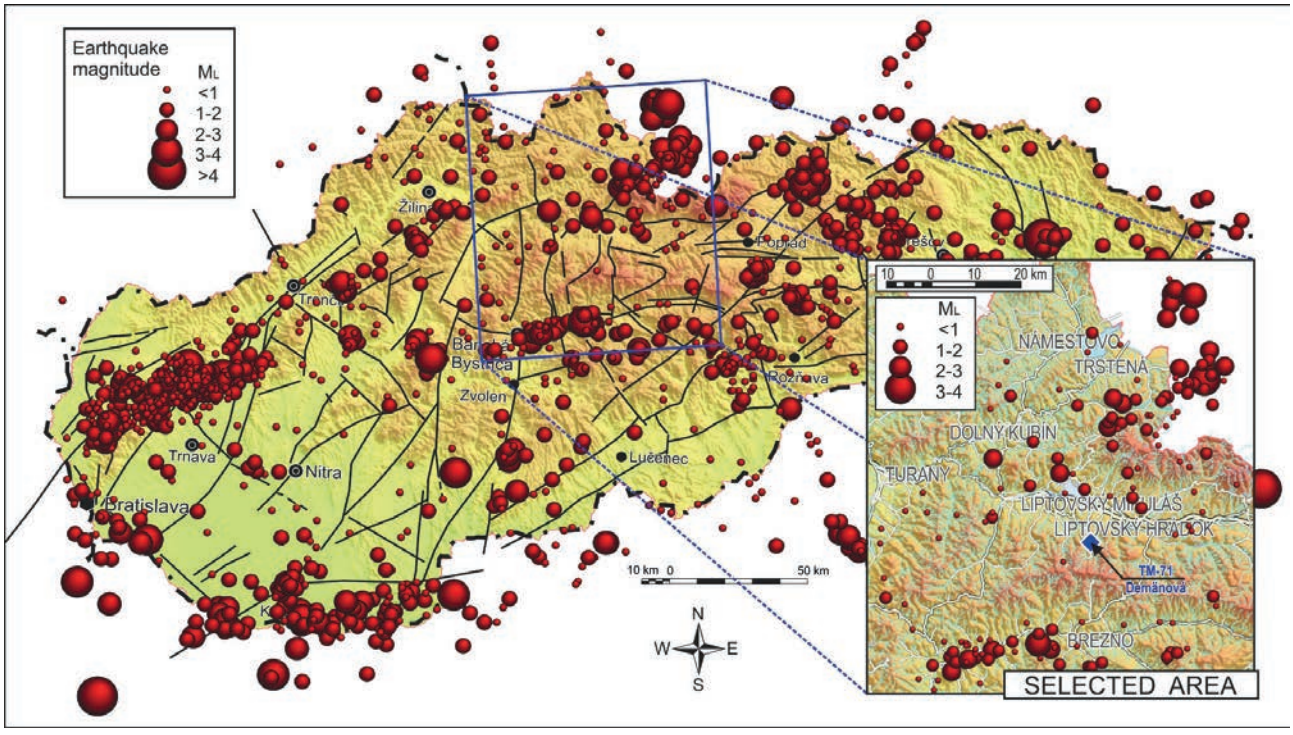

Fig. 11. Observed earthquakes in the territory of Slovakia within the period 2000–2023 with selected ones in the Demänová region (processed using the data from https://dionysos.geology.sk/cmsgf).

Tab. 4

List of seismic events with M_L > 1.5 and epicentral areas in the broader vicinity of Demänová

Date and time of earthquake	Magnitude [M_L]	Epicentre coordinates [X_WGS84 / Y_WGS84]	Epicentral region	Monitoring stage
14 Dec 2002 – 00:27	2.4	49.160 / 19.270	Banská Bystrica and surroundings	A
10 Jan 2004 – 07:43	2.2	48.770 / 19.310	Banská Bystrica and surroundings	B
12 Jun 2004 – 09:59	2.2	48.720 / 19.190	Polish-Slovak border area	B
30 Nov 2004 – 17:18	4.4	49.350 / 19.910	Polish-Slovak border area	B
01 Dec 2004 – 23:25	2.6	49.480 / 19.850	Polish-Slovak border area	B
02 Dec 2004 – 18:25	3.2	49.520 / 19.800	Polish-Slovak border area	B
09 Dec 2004 – 01:09	2.9	49.500 / 19.790	Polish-Slovak border area	B
11 Dec 2004 – 17:25	2.3	49.380 / 19.970	Polish-Slovak border area	B
13 Dec 2004 – 03:29	2.5	49.410 / 19.920	Polish-Slovak border area	B
13 Dec 2004 – 00:05	2.3	49.470 / 19.780	Polish-Slovak border area	B
23 Jan 2005 – 23:33	2.5	49.530 / 19.800	Polish-Slovak border area	B
29 Jan 2005 – 17:16	3.0	49.520 / 19.860	Polish-Slovak border area	B
07 Feb 2005 – 06:08	1.8	49.380 / 19.920	Polish-Slovak border area	B
01 May 2005 – 16:17	1.7	49.200 / 19.930	Polish-Slovak border area	B
02 Jun 2005 – 07:43	2.7	49.370 / 19.830	Polish-Slovak border area	B
07 Jun 2005 – 11:00	2.0	48.780 / 19.490	Brezno and surroundings	B
24 Aug 2005 – 15:46	1.7	49.380 / 19.900	Polish-Slovak border area	B
10 May 2008 – 17:33	1.5	49.310 / 19.790	Orava	C
27 May 2015 – 14:39	1.9	49.110 / 19.560	Liptovský Mikuláš and surroundings	E
03 Nov 2015 – 13:02	3.2	48.790 / 19.450	Brezno and surroundings	E
15 Apr 2017 – 04:12	1.6	48.760 / 19.190	Banská Bystrica and surroundings	E
14 Nov 2018 – 23:16	2.1	49.290 / 19.660	Orava	E
13 Apr 2019 – 04:04	1.6	48.780 / 19.850	Brezno and surroundings	E
15 Sep 2019 – 00:44	2.1	49.300 / 19.630	Orava	E
31 Aug 2020 – 07:50	1.6	48.750 / 19.610	Brezno and surroundings	E
22 Mar 2021 – 17:29	2.1	49.140 / 19.480	Liptovský Mikuláš and surroundings	E
29 Jul 2021 – 07:58	1.9	48.760 / 19.650	Brezno and surroundings	E
13 Oct 2021 – 01:02	1.8	48.810 / 19.450	Brezno and surroundings	E
06 Apr 2022 – 17:04	2.1	48.748 / 19.238	Banská Bystrica and surroundings	E
09 Oct 2023 – 18:23	4.9	49.058 / 21.717	Veľká Domaša	E

speleothems (Fig. 2) was caused by strong earthquakes. Based on the dating of these disruptions and fractures, along with mathematical modelling and other scientific methods, the probable source of the seismic activity was identified as the Sub-Tatra Fault, located approximately 17.5 km from the cave (Szczygieł et al., 2021).

To explore potential links between block displacements and seismic activity at the Demänovská Cave of Liberty, measured TM-71 data were compared with records of seismic events detected by the National Seismic Network of the Earth Science Institute of the Slovak Academy of Sciences (ESI SAS) in Bratislava. During the TM-71 monitoring period, over 1 600 earthquakes of various magnitudes and epicentral locations were recorded across Slovakia and surrounding areas (https://dionysos.geology.sk/cmsgf/). However, none of these events had epicentres located directly in the vicinity of Demänová or along the aforementioned Sub-Tatra Fault (Fig. 11).

To investigate further, approximately 150 seismic events were selected – mostly minor earthquakes with epicentres in the broader vicinity of the monitored site. Several more distant but stronger events were also considered. The local magnitudes (M_L) of these selected earthquakes ranged from nearly undetectable to a maximum of 4.9 (Veľká Domaša – Ďapalovce, October 9, 2023). Table 4 lists selected seismic events with M_L > 1.5, including

their assignment to specific stages of recorded neotectonic activity, showing a similar pattern on the monitored fault.

Synthesis and Interpretation of TM-71 Measurements

The Demänová Valley area, based on available data during the monitoring period, appeared to be seismically quiet, classifying it as an aseismic zone.

As previously mentioned, throughout the entire period of monitoring duration at this site using the TM-71, no earthquake has been recorded with a calculated epicentral area located in the immediate vicinity of the monitored site.

Nonetheless, a certain correlation can be observed between some seismic events with broader epicentral regions and variations in the measured data. Such changes may include, for example, abrupt jumps in one or more curves simultaneously, or reversals in long-term trends, for which no alternative explanation is acceptable. These moments – the instances of change – along with recorded seismic events, form the basis for interpreting the temporal characteristics of neotectonic activity at the measured fault.

Based on the synthesis of all data, the entire monitoring period has been subdivided into shorter temporal segments characterised by consistent or similar expressions across all monitored indicators during each phase. Within the Demänovská Cave of Liberty site, phases A–E were delineated for interpretative purposes (see Fig. 12).

The first interpreted period (A) is temporally bounded by an earthquake in the Orava Basin region (M_L = 2.4) recorded on December 14, 2002. Approximately at this time, a sudden change in trend orientation was observed on the Y- and Z-curves, and a peak at –0.05 degrees was registered on the XY rotation curve. This event may not necessarily relate to tectonic activity; however, it is noteworthy that in the subsequent years, only minimal changes occurred on this curve. The X-component displays a declining trend, which continues – albeit with a slightly altered slope – throughout the subsequent period (B). In contrast, the Y and Z curves show a reversal to a mildly increasing trend at the beginning of phase B, diverging from the development seen in the X-component. Rotations in the horizontal (XY) plane exhibit a slight increasing trend, while those in the vertical (XZ) plane show a subtle decrease.

The entire period until May 2008 can be considered relatively stable, with no significant changes. Seismically, numerous moderate to weak earthquakes were recorded during this phase (Tab. 4), predominantly with epicentres north of the site, some near the Polish-Slovak border. Notably, the earthquake on November 30, 2004 (M_L = 4.4) did not visibly affect the recorded data.

During this period, the activity along the fault can be characterised as a sinistral subsidence of the mobile block accompanied by fault opening, with horizontal block rotation resulting in the crack opening towards the southeast, and vertical rotation contributing to the upward opening of the crack (Fig. 13).

Phase C, by contrast, can be described as a period of increased instability based on the observed data. It began with a moderate earthquake (M_L = 1.5) on May 10, 2008, centred near Orava. From May 2008 to July 2009, significant changes occurred on all curves. The most pronounced ones were in the rotation curves – XY rotations exhibited a rapid increase, rising sixfold in this short interval, while XZ rotations declined sharply, with a decrease of nearly 0.15 degrees. These values suggest modifications in the stress state along the tectonic line. The Z-curve initially decreased, then sharply increased by nearly +0.2 mm, indicating a vertical mutual displacement of the blocks relative to each other by 0.2 mm – a potentially macroscopically observable phenomenon, particularly on stalactite formations.

The X-curve during this phase shows a sharp rise initially (possibly associated with an earthquake, similar to other curves), followed by a relatively steady upward trend that persisted until 2015 without responding to seismic events. This indicates a gradual closing of the crack at approximately 0.01 mm per year – which is a minor value. **The activity during this period can thus be interpreted as a displacement of the moving block (or relative mutual displacement of the blocks to each other) along the fault line with simultaneous closing of the crack, without substantial lateral movement, but coupled with a right-lateral (clockwise) rotation in the horizontal plane and a left-lateral (counterclockwise) rotation vertically.**

Subsequent Period D (July 2009 – April 2015) showed no changes in the prevailing trends of the X and Y curves. The X-component showed a slightly increasing trend, indicating crack closing, while the Y-component remained stable – apart from a sudden sinistral shift of approximately 0.05 mm at the end of the phase. Almost all curves (with the exception of XY rotation) exhibited distinct stepwise displacements in the positive direction at the end of this phase. The Z-component reversed orientation at the beginning of the period, indicating uplift of the block (reverse faulting), and returned to its original value through a sharp shift at the end of the phase.

The most pronounced effects were recorded in the rotation curves. At the beginning of the period, the XZ rotation trend reversed sharply and continued to increase significantly throughout. A sudden increase of nearly 0.2° in the positive direction occurred at the end of the period. The horizontal (XY) rotation curve stagnated at first, but between 2013 and 2014, there was a slight left-lateral

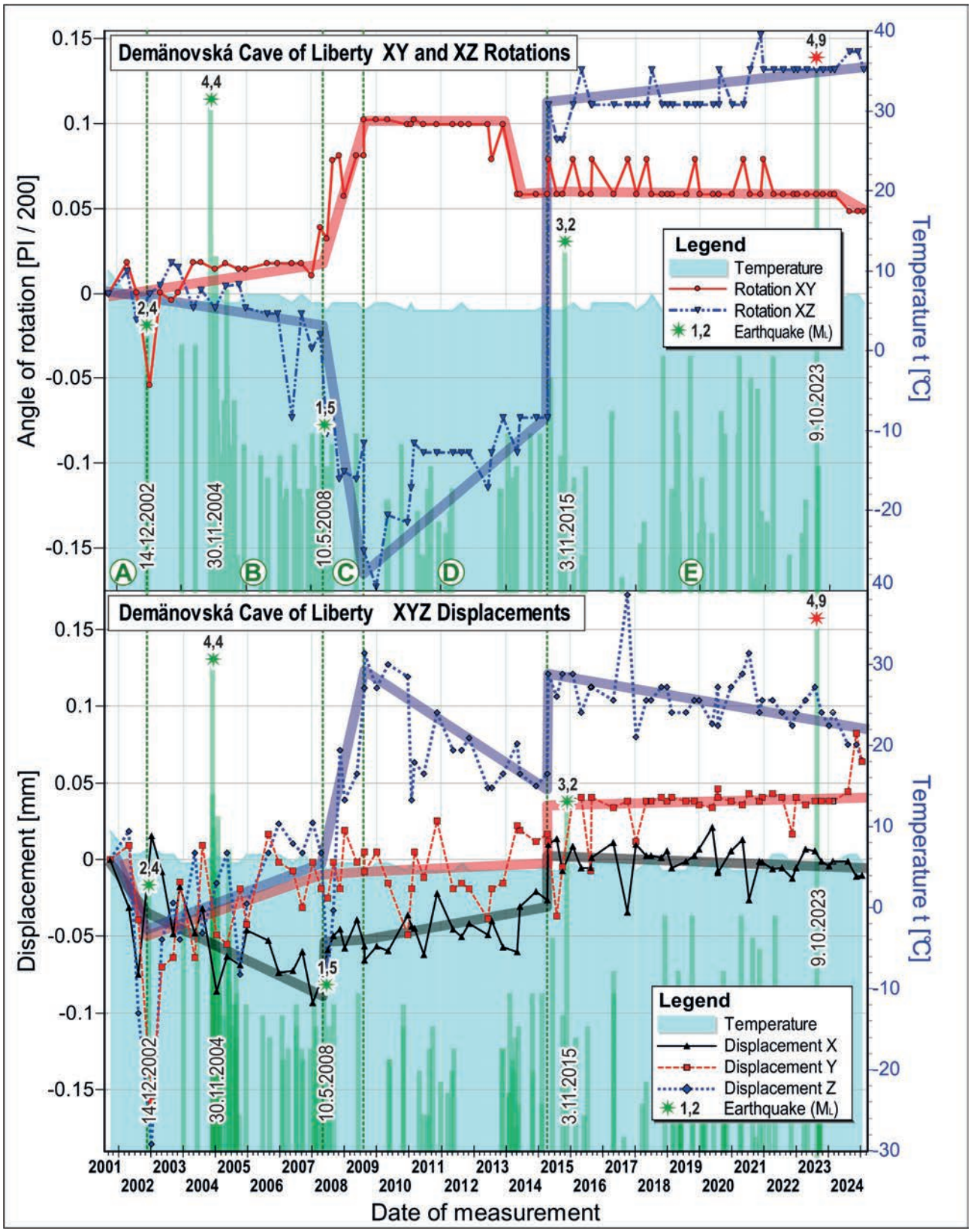

Fig. 12. Displacement records (X, Y, Z) and rotations (XY – horizontal, XZ – vertical) of tectonic blocks detected by the TM-71 extensometer installed inside the Demänovská Cave of Liberty

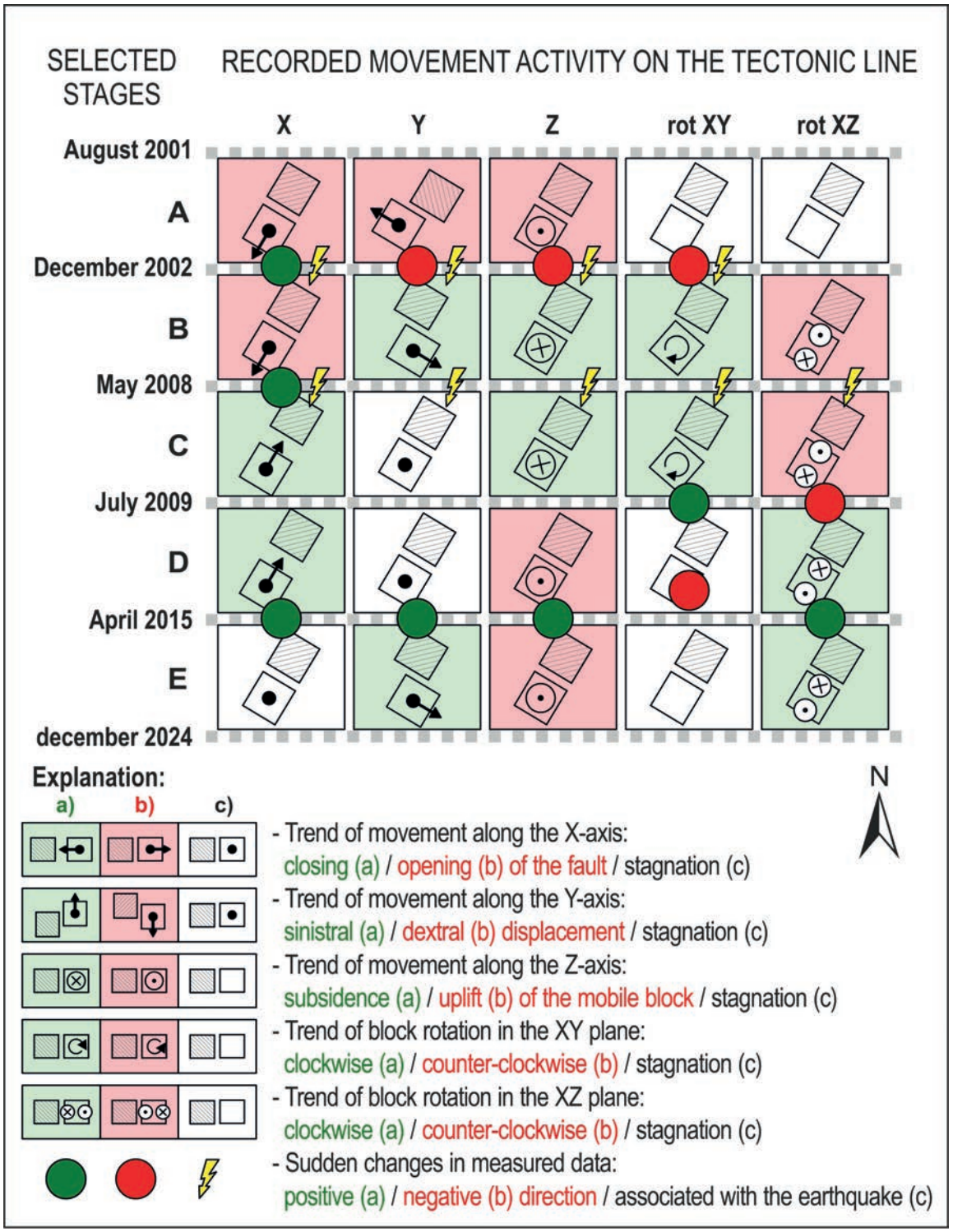

Fig. 13. Overview of neotectonic activity during the individual interpreted phases.

rotation of approximately 0.05°, followed by continued stagnation until the end of the observation period. **The overall movement in this phase can be characterised as uplift of the mobile block accompanied by crack closing, with no significant lateral movement, and vertical rotation toward the crack (closing of the upper part of the crack, opening of the lower part).**

Final Period E (April 2015 – December 2024) was markedly more stable. This entire interval may be characterised as stable, without significant changes. Most curves show stagnation or only slight decreasing (Z) or increasing (Y and XZ) trends. Early in this period (3 November 2015), a stronger earthquake was recorded near Brezno, which may correlate with a change in the Y-curve – namely, a sinistral shift of about 0.05 mm, after which the curve remained notably stable until the present.

A strong earthquake (M_L = 4.9) recorded near Veľká Domaša (Ďapalovce) on October 9, 2023 did not produce any observable response in the data (Fig. 12). **The movements observed in this period are characterised by uplift, sinistral shift, and vertical rotation toward the crack (closing of the upper side, opening of the lower side).**

Summary of Results

Based on the measured data, neotectonic activity along fault structures in the Demänovská Cave of Liberty is not particularly intense, but it is nonetheless present and, under the given conditions, measurable. It is important to emphasise that the displacements are very small – close to the detection threshold of the extensometer – and that the data would likely be unreliable in less stable climatic conditions. Therefore, it is concluded that the threat to human safety in this location from neotectonic activity is considered minimal.

From the perspective of the nature of monitored movements along the tectonic line, it can be concluded that displacements are generally not continuous but more often occur in sudden jumps and may sometimes be associated with seismic events. Moreover, the direction of movement does not necessarily correspond to the long-term trend and may exhibit oscillations around a mean value (i.e., periodic shifts in movement direction). During the monitoring period, several changes were observed that served as the basis for dividing the data into temporal segments A–E, within which the character of the recorded data related to neotectonic activity remains consistent (Fig.12). The periods showing the most pronounced manifestations of neotectonic activity in the character of the recorded curves at the Demänovská Cave of Liberty site are Phase C and the short interval between Phases D and E. Interestingly, neither of these episodes appears to be associated with any seismic event.

Szczygieł et al. (2021) interpreted numerous broken and fallen dripstones and flowstones in the Čarovná chodba Passage as the result of oscillation accompanying fault reactivation. The healed speleothems observed in the fractured deformation of older speleothems, especially columns and flowstones, are undoubtedly associated with ancient seismotectonic activity (Sala et al., 2022).

Acknowledgements

The authors would like to express their thanks to EC and the Ministry of Environment of the Slovak Republic for funding several scientifically contributing geological and tectonic projects, including the project entitled *Monitoring System of the Environment of the Slovak Republic – Partial Monitoring System – Geological Factors*.

References

Bada, G., 1999: Cenozoic stress field evolution in the Pannonian Basin and surronding orogens. Academisch proefschrift. *Vrije Universiteit Amsterdam*, 1 – 187.

Bella, P., Haviarová, D., Kováč, Ľ., Lalkovič, M., Sabol, M., Soják, M., Struhár, V., Višňovská, Z. & Zelenka, J., 2014: Jaskyne Demänovskej doliny. *Liptovský Mikuláš, ŠOP SR, SSJ,* 200 pp.

Bella, P., 2016: Multi-levelled cave system and associated morphological segments in the contact middle-mountain karst: the case study from the Demänová Caves, the Nízke Tatry Mts. *Geomorphica Slovaca et Bohemica*, 16, 1, 13 p.

Bezák, V., Broska, I., Ivanička, J., Reichwalder, P., Vozár, J., Polák, M., Havrila, M., Mello, J., Biely, A., Plašienka, D., Konečný, V., Lexa, J., Kaličiak, M., Žec, B., Vass, D., Elečko, M., Janočko, J., Pereszlényi, M., Marko, F., Maglay, J. & Pristaš, J., 2004: Tectonic Map of Slovak Republic 1 : 50 000. *Bratislava, Ministry of Environment of the Slovak Republic – State Geological Institute of Dionýz* Štúr.

Biely, A., Bezák, V., Bujnovský, A., Vozárová, A., Klinec, A., Miko, O., Halouzka, R., Vozár, J., Beňuška, P., Hanzel, V., Kubeš, P., Liščák, P., Lukáčik, E., Maglay, J., Molák, B., Pulec, M., Putiš, M. & Slavkay, M., 1997: Explanation to the geological map of the Nízke Tatry Mountains 1 : 50 000. *Bratislava, GS SR, Dionýz Štúr Publisher.*

BIPM, IEC, IFCC, ISO, IUPAC, IUPAP, OIML, 2008: Evaluation of measurement data – Guide to the expression of uncertainty in measurement (GUM 1995 with minor corrections). JCGM 100. *Joint Committee for Guides in Metrology*, 120 p.

Briestenský, M., Stemberk, J. & Petro, Ľ., 2007: Displacements registered around March 13, 2006 Vrbové earthquake, M=3.2 (Western Carpathians). *Geologica Carpathica*, 58, 487–493.

Briestenský, M., Košťák, B., Stemberk, J., Petro, L., Vozár, J. & Fojtíková, L., 2010: Active tectonic fault microdisplacement analyses: a comparison of results from surface and underground monitoring in western Slovakia. *Acta Geodynamica et Geomaterialia*, 7, 4 (160), 387–397.

Briestenský, M., Košťák, B., Stemberk, J. & Vozár, J., 2011: Long-term slope deformation monitoring in the high

mountains of the Western Carpathians. *Acta Geodynamica et Geomaterialia*, 8, 4 (164), 403–412.

Briestenský, M., Hochmuth, Z., Littva, J., Hók, J., Dobrovič, R., Stemberk, J., Petro, Ľ. & Bella, P., 2018: Present-day stress orientation and tectonic pulses registered in the caves of the Slovenský kras Mts. (South-Eastern Slovakia). *Acta Geodynamica et Geomaterialia*, 15, 2, 93–103. https://doi.org/ 10.13168/AGG.2018.0007.

Slovak speleological society, 2025: The list of the longest caves in Slovakia as of March 10, 2025. *Bulletin of the Slovak Speleological Society*, 56, 1, 110.

Droppa, A., 1957: Demänovské Caves, Karst Landforms of the Demänová Valley. *Bratislava, Slovak Academy of Sciences,* 289 pp. (in Slovak with Russian and German Summary).

Droppa, A., 1972: Geomorfologické pomery Demänovskej doliny. *Slovenský kras*, 10, 9–46.

Hochmuth, Z., Briestenský, M., Zacharov, M., Stemberk, J., Petro, Ľ., Littva, J., Bella, P., Gaál, Ľ., Hraško, Ľ. & Stankovič, J., 2020: Monitoring mikropohybov v jaskyniach Slovenského a Ochtinského krasu [Microdisplacements monitoring in the caves of Slovak and Ochtiná karsts]. *Slovenský kras*, 58, 2, 169–180.

Hók, J., Bielik, M., Kováč, P. & Šujan, M., 2000: Neotectonic character of Slovakia (in Slovak with English summary). *Mineralia Slovaca*, 32, 459–470.

Jánová, V., Liščák, P. (eds.), Kopecký, M., Bednarik, M., Šimeková, J., Ondrášik, M., Pauditš, P., Tupý, P., Petro, Ľ., Ondrejka, P., Greif, V. & Ondrus, P., 2021: Zosuvy na Slovensku. *Banská Bystrica, Slovenská agentúra životného prostredia*, 166–169.

Košťák, B., 1969: A new device for in-situ movement detection and measurement. Experimental Mechanics. *SESA (American Society for Experimental Stress Analysis) Journal,* 9, 374–379.

Maglay, J., Halouzka, R., Baňacký, V., Pristaš, J. & Janočko, J., 1999: Neotektonická mapa Slovenska. *Bratislava, Ministerstvo životného prostredia SR, GS SR.*

Mann, H. B, 1945: Nonparametric tests against trend. Econometrica. *Econometrica*, 13, 245–259.

Ondrejka, P., Wagner, P., Petro, Ľ., Žilka, A., Balík, D., Iglárová, Ľ. & Fraštia, M., 2014: Main results of the slope deformations monitoring. *Slovak Geological Magazine,* 14, 89–114.

Ondrus, P. (ed.), 2025: Čiastkový monitorovací systém [online]. *Bratislava, Štátny geologický ústav Dionýza Štúra.* Available online: https://dionysos.geology.sk/cmsgf/.

Petro, Ľ., Košťák, B., Polaščinová, E. & Spišák, Z., 1999. Block movements monitoring in the Slanské vrchy Mts. (Eastern Slovakia). *Mineralia Slovaca*, 31, 549–554 (in Slovak with English summary).

Petro, Ľ., Vlčko, J., Ondrášik, R. & Polaščinová, E., 2004a: Recent tectonics and slope failures in the Western Carpathians. *Engineering Geology*, 74, 103–112.

Petro, Ľ., Bella, P., Polaščinová, E., Hók, J. & Stercz, M., 2004b: Monitoring of tectonic movements in the Demänovská Cave of Liberty. *Aragonit*, 9, 26–29 (in Slovak with English Summary).

Petro, Ľ., Košťák, B., Stemberk, J. & Vlčko, J., 2011a: Geodynamic reactions to recent tectonic events observed on selected sites monitored in Slovakia. *Acta Geodynamica et Geomaterialia*, 8, 4 (164), 453–467.

Petro, Ľ., Bóna, J., Kováčik, M., Fussgänger, E., Antonická, B. & Imrich, P., 2011b: The Cave under the Spišská hill: Preliminary results of the block movements. *Mineralia Slovaca*, 43, 121–128.

Petro, Ľ., Brček, M., Vlčko, J., Šimková, I., Balík, D. & Žilka, A., 2012: Stability of selected historical objects in Slovakia: Monitoring results. *Mineralia Slovaca,* 44, 403–422 (in Slovak with English summary).

Piccardi, L. (ed.), 2006: 625 – 3-D Monitoring of Active Tectonic Structure. *Brussels, COST.* Available online: https://www.cost.eu/actions/625/.

Pokorný, M., 1952: Vznik a vývoj starších prostor jeskyň Demänovských. *Časopis Moravského musea v Brně*, 37, 13–51 (in Czech with English summary).

Rowberry, M. D., Kriegner, D., Holy, V., Frontera, C., Llull, M., Olejnik, K. & Marti, X., 2016: The instrumental resolution of a moiré extensometer in light of its recent automatisation. *Measurement*, 90, 237–243. https://doi.org/10.1016/j.measurement.2016.05.048.

Sala, P., Bella, P., Szczygieł, J., Wróblewski, W. & Gradziński, M., 2022: Healed speleothems: A possible indicator of seismotectonic activity in karst areas. *Sedimentary Geology*, 430, 106105. https://doi.org/10.1016/j.sedgeo.2022.106105.

Sasvári, Á. & Baharev, A., 2014: SG2PS (Structural Geology to Post Script Converter) – A graphical solution for brittle structural data evaluation and paleostress calculation. *Computers & Geosciences*, 66, 81–93.

Sen, P. K., 1968: Estimates of the Regression Coefficient Based on Kendall's Tau. *Journal of the American Statistical Association*, 63, 324, 1379–1389.

Stercz, M., 2021: MSDilat V3.1 – application for computer processing of the TM-71 3D measurements. *Prepared by M. Stercz in Delphi language for MS Windows platform.*

Stercz, M., Grega, D., Petro, Ľ., Hók, J., Németh, Z., Stemberk, J. & Bednarik, M., 2025: 3D Long-Term Monitoring of Recent Tectonic Activity in the Branisko Tunnel (Eastern Slovakia). *Geologica Carpathica*, 76, 1, 55–67. https://doi.org/10.31577/GeolCarp.2025.04.

Szczygieł, J., Gradziński, M., Bella, P., Hercman, H., Littva, J., Mendecki, M., Sala, P. & Wroblewski, W., 2021: Quaternary faulting in the Western Carpathians: Insights into paleoseismology from cave deformations and damaged speleothems (Demänová Cave System, Low Tatra Mts). *Tectonophysics*, 820, 229111. https://doi.org/10.1016/j.tecto. 2021.229111.

Vlcko, J. & Petro, L., 2002. Monitoring of subgrade movements beneath historic structures. In: Van Roy, J. L. & Jermy, C. A. (Eds.): *Proc. of 9th Inter. Congress IAEG, Durban, South Africa*, 1432–1437.

Wagner, P., Iglárová, Ľ. & Petro, Ľ., 2000: Methodology and some results of slope movement monitoring in Slovakia. *Mineralia Slovaca*, 32, 359–367.

Dlhodobé 3D monitorovanie recentnej tektonickej aktivity v Demänovskej jaskyni Slobody

Práca sa zaoberá analýzou údajov takmer 24-ročného monitorovania tektonických pohybov pozdĺž neotektonickej poruchy v Demänovskej jaskyni Slobody. Posuny a rotácie na poruche boli merané pomocou mechanicko-optického 3D extenzometra TM-71. Výsledky meraní podrobené štatistickej analýze ukázali trend v dvoch zložkách priestorového vektora pohybu – vo vertikálnej (Z) a v horizontálnej (Y), ktorá je kolmá na smer sklonu zlomu. Nedávna aktivita pozdĺž zlomu odráža pôsobenie recentného napäťového poľa a seizmickú aktivitu v rámci Západných Karpát. Štúdia skúma aj vzťah medzi pohybmi zaznamenanými TM-71 a seizmickými udalosťami v širšom okolí jaskyne.

Na základe nameraných údajov je neotektonická aktivita pozdĺž zlomových štruktúr v Demänovskej jaskyni Slobody nízka, ale za daných podmienok merateľná. Posuny sú veľmi malé, blízko detekčnej hranice extenzometra. V menej stabilných klimatických podmienkach by údaje pravdepodobne neboli spoľahlivé. Zistená neotektonická aktivita nepredstavuje žiadne riziko z hľadiska bezpečnosti jaskynných priestorov.

Z hľadiska povahy monitorovaných pohybov pozdĺž tektonickej línie možno konštatovať, že posuny vo všeobecnosti nie sú kontinuálne, ale častejšie sa vyskytujú v náhlych skokoch a niekedy môžu súvisieť so seizmickými udalosťami. Navyše, smer pohybu nemusí nevyhnutne zodpovedať dlhodobému trendu a môže vykazovať oscilácie okolo strednej hodnoty (t. j. periodické posuny v smere pohybu).

Počas monitorovacieho obdobia bolo pozorovaných niekoľko zmien, ktoré slúžili ako základ na rozdelenie údajov do časových segmentov A – E. V rámci nich charakter zaznamenaných údajov týkajúcich sa neotektonickej aktivity zostáva konzistentný (obr. 12). Obdobia s najvýraznejšími prejavmi neotektonickej aktivity v charakteristike zaznamenaných kriviek v Demänovskej jaskyni Slobody sú fáza C a krátky interval medzi fázami D a E. Nezdá sa, že by niektorá z týchto epizód bola spojená so seizmickou udalosťou.

Doručené / Recieved: 18. 6. 2025
Prijaté na publikovanie / Accepted: 1. 9. 2025